Development of a prediction model for the risk of recurrent laryngeal nerve lymph node metastasis in thoracolaparoscopic esophagectomy with cervical anastomosis

Guoqing Zhang[1], Yuanqi Li[2], Qian Wang[3], Huiwen Zheng[3], Lulu Yuan[1], Zhen Gao[1], Jindong Li[1], Xiangnan Li[1], Song Zhao[1]

[1]Department of Thoracic Surgery, First Affiliated Hospital of Zhengzhou University, Zhengzhou, China; [2]Xiangya School of Public Health, Central South University, Changsha, China; [3]The Nursing Department, First Affiliated Hospital of Zhengzhou University, Zhengzhou, China;

Contributions: (I) Conception and design: G Zhang, Y Li, Q Wang, H Zheng, J Li, X Li, S Zhao; (II) Administrative support: S Zhao; (III) Provision of study materials or patients: Q Wang, H Zheng, J Li, X Li, S Zhao; (IV) Collection and assembly of data: G Zhang, Y Li, L Yuan, Z Gao; (V) Data analysis and interpretation: G Zhang, Y Li; (VI) Manuscript writing: All authors; (VII) Final approval of manuscript: All authors.

Correspondence to: Jindong Li; Song Zhao; Xiangnan Li. Department of Thoracic Surgery, First Affiliated Hospital of Zhengzhou University, No. 1 Jian She Road, Zhengzhou 450052, China. Email: 13598820589@163.com; zhaosong@zzu.edu.cn; lxn-2000@163.com.

Background: There are no effective preoperative diagnostic measures to predict the probability of left and right recurrent laryngeal nerve (RLN) lymph node (LN) metastasis using preoperative clinical data in patients undergoing thoracolaparoscopic esophagectomy with cervical anastomosis.

Methods: We retrospectively reviewed the clinical data of 1,660 consecutive patients with thoracic esophageal cancer who underwent esophagectomy with cervical anastomosis at the Department of Thoracic Surgery at the First Affiliated Hospital of Zhengzhou University between January 2015 and December 2020.

Results: A total of 299 and 343 patients who underwent left (Cohort 1) and right (Cohort 2) RLN LN dissection were included in the final analyses. The analyses were conducted within each cohort. Among the 299 patients in Cohort 1, left RLN LN involvement was found in 41 patients (13.7%). A multivariable analysis showed that age, tumor location, and short axis were significantly associated with RLN LN metastasis (all P<0.05). Among the 343 patients in Cohort 2, right RLN LN involvement was found in 65 patients (19.0%). A multivariable analysis showed that computed tomography (CT) appearance, tumor location, long axis, and short axis were significantly associated with RLN LN metastasis (all P<0.05). Based on the results of the multivariable analyses, we constructed nomograms that could estimate the probability of RLN LN metastasis. Finally, we stratified the 2 cohorts into risk subgroups using a recursive partitioning analysis (RPA). The risk of left and right RLN LN metastasis was found to be 9.3% and 7.5%, 27.3% and 21.4%, and 52.4% and 47.3% for the low-risk, intermediate-risk, and high-risk groups, respectively.

Conclusions: Our nomograms and RPAs appear to be suitable for the risk stratification of left and right RLN LN metastasis in patients undergoing thoracolaparoscopic esophagectomy with cervical anastomosis. This tool could be used to help clinicians to select more effective locoregional treatments, such as surgical protocols and radiation area selection.

Keywords: Esophageal cancer; lymphadenectomy; recurrent laryngeal nerve lymph node (RLN LN); nomogram; recursive partitioning analysis

Page 2 of 13

Zhang et al. Risk stratification of lymph node metastasis

Introduction

The reported rates of metastasis to the recurrent laryngeal nerve (RLN) lymph nodes (LNs) in esophageal cancer has varied in previous studies, ranging from 18% to as high as 63% (1-7). Studies have shown the importance of RLN LN dissection. Chao et al. (8) found that the dissection of bilateral RLN LNs results in a 15% decrease in the superior mediastinum recurrence rate. Further, some studies have shown that the dissection of bilateral RLN LNs was significantly beneficial for overall survival (9,10). Additionally, other studies have demonstrated that RLN LNs are important indicators for predicting LN metastasis in the cervical area and selected patients may benefit from three-field dissection (5,6,11). Thus, preoperative RLN LN evaluation is clinically significant in helping clinicians select more effective locoregional treatments, such as surgical protocols and radiation area selection.

The 2 RLNs are not symmetrical; the right RLN LNs collect a larger volume of lymphatic drainage from the esophagus and possibly from other organs, while the left RLN LNs collect little drainage from the esophagus (10). Thus, the left and right RLN LNs may possess different anatomical characteristics and metastasis patterns. Kanemura et al. (12) demonstrated that right RLN LNs tend to be larger and round than left RLN LNs. In relation to the metastasis rate between the left and right RLN LNs, the available data are inconsistent. Udagawa et al. reported that right RLN LNs had a higher metastasis rate than left RLN LNs (13). However, other studies have reported identical metastasis rates between left and right RLN LNs (9,12). High-resolution computed tomography (CT) scans have facilitated the identification of relatively small LN metastases that might have been previously diagnosed only through pathological examinations. In previous studies, LNs with a short-axis diameter >l0 mm (14) or a long/short-axis diameter ratio not exceeding 1.52 (LNs tend to be round) (15) were suspicious of tumor involvement. However, LNs at different anatomical sites have different drainage areas, resulting in different sizes of LNs.

Several studies have built models to predict RLN LN metastasis in thoracic esophageal cancer. However, not all the included variables used by Liu et al. (16) and Yu et al. (17) could be obtained preoperatively, which may limited the clinical application of the models in their preoperative decision making. Li et al. (18) concluded a 6.5 mm cutoff (short diameter) can be applied to clinically predict lymph node metastasis along the right RLN. However, the authors did not further discuss the differences between the left and right RLN LN metastasis. Thus, in this study, we investigated the risks and internal validation of bilateral RLN LNs according to preoperative CT scans and pathological examination findings to assist clinicians to develop treatment strategies when patients receive locoregional treatments, such as surgery or radiation.

We present the following article in accordance with the TRIPOD reporting checklist (available at https://dx.doi.org/10.21037/atm-21-2374).

Methods

Data source and case selection

A total of 1,660 patients with esophageal cancer underwent an esophagectomy with cervical anastomosis at the Department of Thoracic Surgery at the First Affiliated Hospital of Zhengzhou University between January 2015 and December 2020. The remaining eligible patients were enrolled in this retrospective study after the application of strict inclusion criteria (see Figure 1). We excluded patients with a history of other malignant diseases or with other concurrent malignant diseases of the esophagus or other organs. We only included patients with squamous cell thoracic esophageal cancer (high-grade intraepithelial neoplasia or carcinoma in situ was excluded) who underwent a R0 thoracolaparoscopic esophagectomy with cervical anastomosis. To obtain data on the long and short axes of the left and right RLN LNs, we excluded patients without contrast-enhanced CT scans (and those who had been scanned at other hospitals). Patients who had received neoadjuvant therapy (chemotherapy, radiotherapy, or chemoradiotherapy) and those without detailed LN grouping were also excluded. The remaining eligible patients were enrolled in this retrospective study. Patients who underwent left and right RLN LN dissection were classified as Cohort 1 and Cohort 2, respectively. All procedures performed in this study involving human participants were in accordance with the Declaration of Helsinki (as revised in 2013). This study was deemed exempt from review by the Zhengzhou University Institutional Review Board (No.: 2021-KY-0397-102) and informed consent was waived because our study was retrospective.

In our study, the tumor location and LN stations were categorized according to the 11th edition of the Japanese Classification of Esophageal Cancer (19,20). The left and right non-RLN are rare anatomical variants associated with arterial anomalies: right aortic arch with anomalous origin of the left subclavian artery (0.05–0.1%), or left aortic arch with anomalous origin of right subclavian artery (0.5–2%)
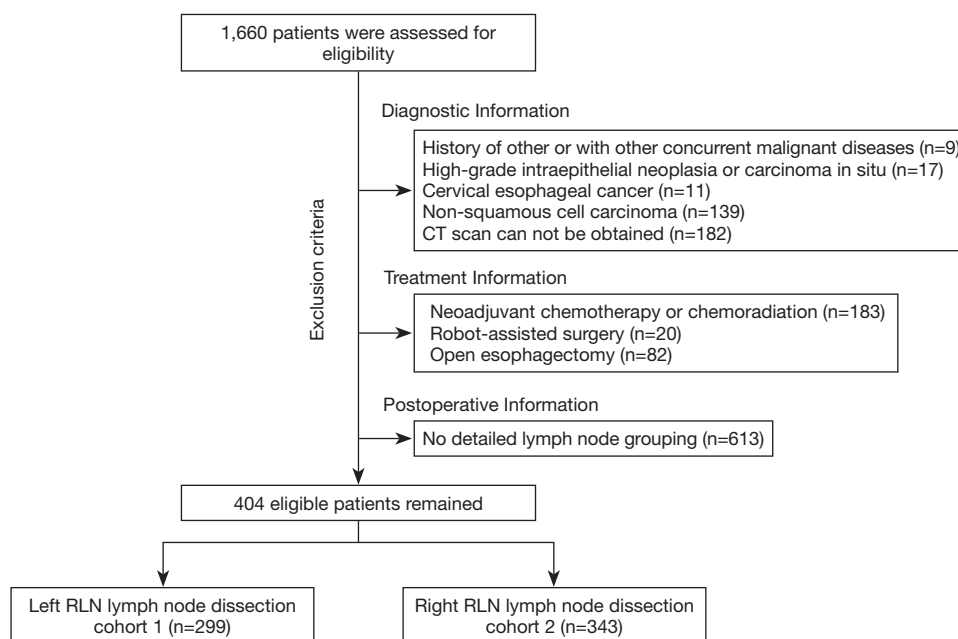
Figure 1 The algorithm used to identify eligible patients in this study. RLN, recurrent laryngeal nerve.

Figure 2 Proposed type of esophageal cancer radiological appearance evaluated by CT. (A) Type 1: mass absent; (B) type 2: eccentric mass; (C) type 3: circumferential mass. CT, computed tomography.

(21,22). Under the circumstances, the left and right RLN are not visible through thoracoscopic surgery. None of our included patients had such deformities. The tumor location within the thoracic esophagus was categorized according to the 8th edition of the American Joint Committee on Cancer (AJCC) staging system. The length of the tumor was determined by gastroscopy. Considering that CT scans have more advantages than endoscopy in evaluating the structure of the esophageal wall, we proposed novel types of esophageal cancer radiological appearances evaluated by CT (see *Figure 2*). CT appearances were defined as follows: (I) type 1, mass absent: the mass is not visible under CT scan; (II) type 2, eccentric mass: focal thickening of the esophageal wall under CT scan; and (III)

type 3, circumferential mass: circumferential diffuse wall thickening of the esophageal wall under CT scan. Based on previous reports, which indicated that metastatic nodes are larger than non-metastatic nodes (23), the most enlarged RLN LNs were identified as potentially malignant on the preoperative CT scans (see *Figure 3*).

On the other hand, RLN LN dissection increases the risk of complications, particularly RLN palsy (RLNP). Studies have reported that the overall incidence of RLNP after esophagostomy ranged from 36% to 58.6%, and 10.7–29.7% of these patients presented with permanent palsy (3,24-26). RLNP increases morbidity, such as hoarseness of voice and aspiration pneumonia, which can be fatal for patients who have undergone esophagostomy

Page 4 of 13

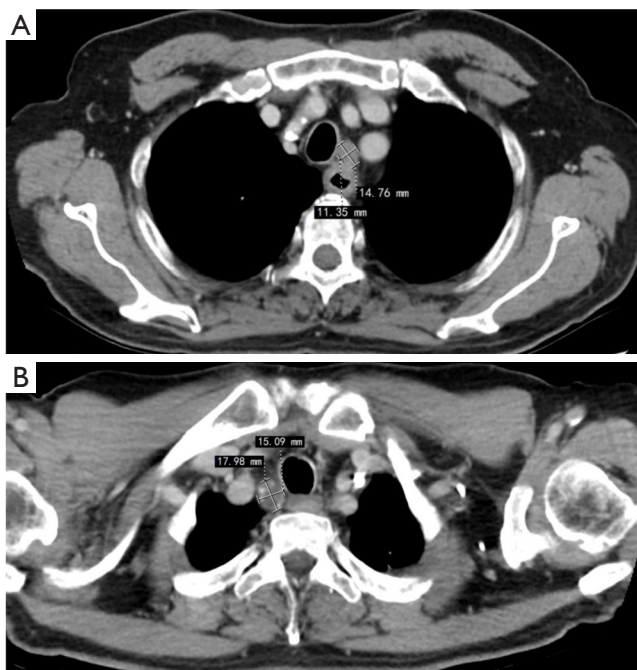Zhang et al. Risk stratification of lymph node metastasis

Figure 3 The long and short axes of the bilateral RLN LNs measured by a contrast-enhanced CT scan. (A) Left RLN LN; (B) right RLN LN. RLN, recurrent laryngeal nerve; LN, lymph node; CT, computed tomography.

(25-27). Technical points of thoracoscopic RLN LN dissection to avoid its complications in our center: (I) dissect bilateral RLN in thoracoscopic left and right RLN LN dissection. The best way to protect the bilateral RLN is to expose them. (II) Avoid the use of energy based devices in a critical area near the RLN. (III) Preserve the vessels and fascia on the surface of the RLN. (IV) Avoid the RLN to be overstretched.

Statistical analysis

Categorical variables were compared using the chi-squared test and are expressed as frequencies (n) and proportions (%). Continuous variables were compared using Student's *t*-test and are expressed as means [and standard deviations (SDs)]. For the long-axis, short-axis and long-to-short-axis ratios, we plotted receiver operating characteristic (ROC) curves in an attempt to find cutoff values to predict metastasis of RLN LNs (*Figure 4*). The maximum value of "sensitivity + specificity – 1" was selected as the optimal cutoff value. Clinically relevant variables with a P value <0.05 in the univariable analysis were included in the multivariable
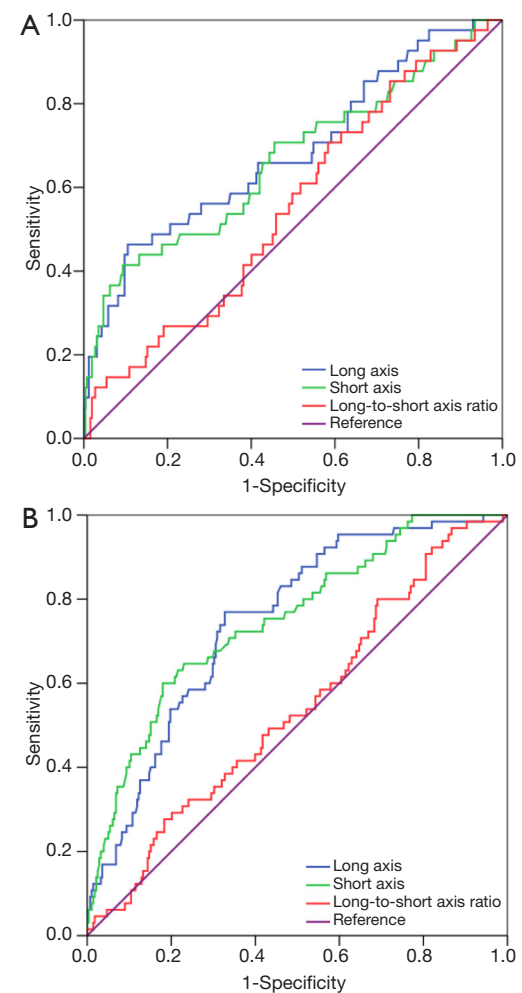

Figure 4 The ROC curve of RLN LN metastasis and LN diameter measured by CT. (A) Left RLN; (B) right RLN. ROC, receiver operating characteristic; RLN, recurrent laryngeal nerve; LN, lymph node; CT, computed tomography.

logistic regression model, and variables with a P value <0.05 were regarded as statistically significant in the final model.

The primary endpoints of this study were left or right RLN LN metastasis, which was evaluated by a postoperative pathological biopsy. A prediction model was constructed based on the final logistic regression model (*Figure 5*). The discrimination of the model was evaluated using the concordance index (c-index). Calibration was evaluated using a calibration plot, which was used to assess the model-predicted probabilities relative to the actual probabilities (*Figure 6A,B*). A decision curve analysis (DCA) was also performed to compare the threshold probabilities and the net benefits that were associated with the nomogram
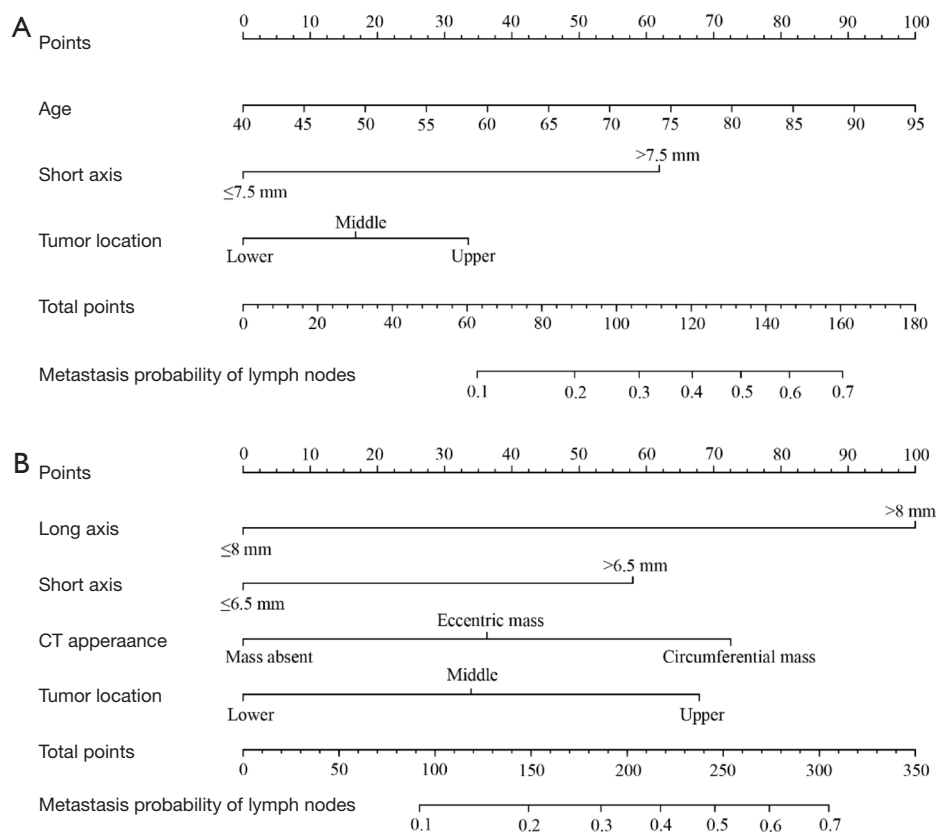
Figure 5 Nomogram for predicting metastasis of RLN LNs. (A) Left RLN LN; (B) right RLN LN. The instructions were as follows: locate a patient's characteristics on the corresponding axis to determine how many points the patient receives. Sum the points allocated to each of the characteristics, and locate this sum on the total points axis. Draw a line straight down to identify the patient's probability of metastasis of left (A) and right (B) RLN LNs. CT, computed tomography; RLN, recurrent laryngeal nerve; LN, lymph node.

(*Figure 6C,D*). A RPA was performed to determine the optimal cutoff points for nomogram-predicted RLN LN metastasis. A RPA was used to objectively divide patients into 2 groups at each step based on the predicted RLN LN metastasis. Based on the RPA, several cutoff points were identified to predict RLN LN metastasis, and the patients were divided into several subgroups based on the risk of RLN LN metastasis (*Figure 7*).

The data were analyzed with SPSS version 22 for Windows (SPSS Inc., Chicago, IL, USA) and R version 3.4 (28). The data sets are available to access upon reasonable request.

Results

Patient characteristics

The clinicopathological characteristics of the cohorts are summarized in *Table 1*. The mean long-axis, short-axis,

and long-to-short-axis ratios of the left RLN LNs were 7.98±0.163, 5.53±0.100 and 1.45±0.017 mm, respectively. By plotting the ROC curves, we concluded that the long-axis and short-axis ratios, rather than the long-to-short–axis ratio, could be used as a diagnostic indicator of RLN LN metastasis (see *Figure 4*). The cutoff values of the long axis and short axis to predict metastasis of the left (right) RLN LNs were 10 mm (8 mm) and 7.5 mm (6.5 mm), respectively (see *Tables 1* and *2*). Detailed information on the ROC curves is set out in *Table 2*.

Risk stratification of left RLN LN metastasis

In Cohort 1, age, tumor location, long axis, and short axis were associated with left RLN LN metastasis (see *Table 3*). The multivariable analysis showed that age, tumor location, and short axis were significantly associated with left RLN LN metastasis (all $P<0.05$) (see *Table 4*). Based on the results of

Page 6 of 13

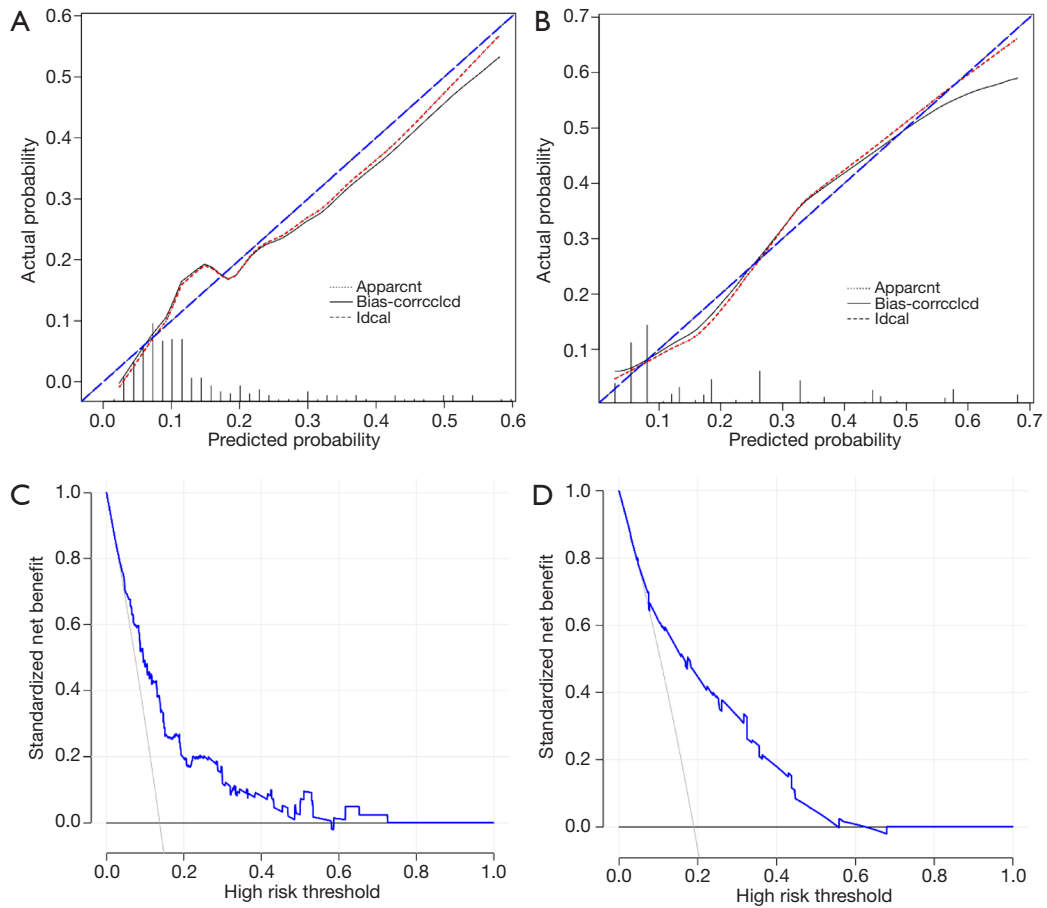Zhang et al. Risk stratification of lymph node metastasis

Figure 6 Evaluation of the nomograms for predicting metastasis of left and right RLN LNs. Calibration plots (A,B) and the decision curve analysis (C,D) of the nomogram for predicting metastasis of left (A,C) and right (B,D) RLN LNs. RLN, recurrent laryngeal nerve; LN, lymph node.
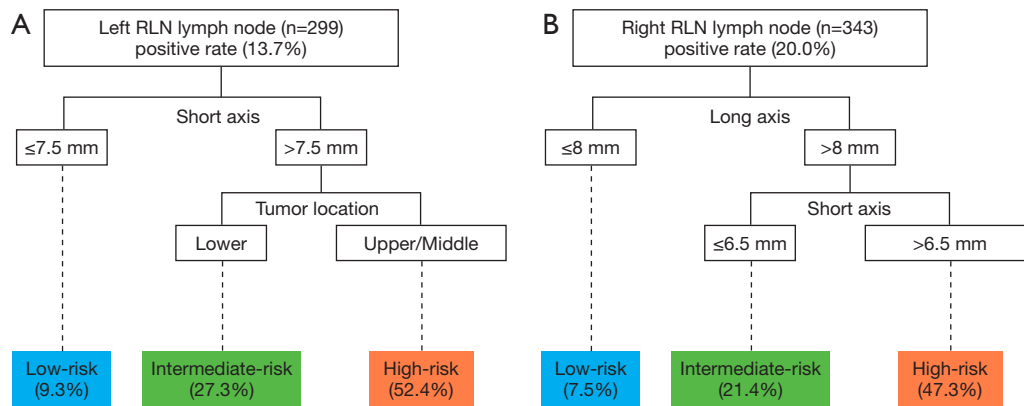

Figure 7 Recursive partitioning analysis for risk stratification according to the probability of bilateral RLN LN metastasis. (A) Left RLN LN; (B) right RLN LN. RLN, recurrent laryngeal nerve; LN, lymph node.

Table 1 Clinical background of the cohorts

Variables	Left RLN LN (n=299)	Right RLN LN (n=343)
Gender, n (%)		
Male	204 (68.2)	229 (66.8)
Female	95 (31.8)	114 (33.2)
Age (y), median (min, max)	65 (40, 94)	65 (44, 86)
BMI mean ± SD	23.68±0.180	23.66±0.170
CT appearance, n (%)		
Mass absent	53 (17.7)	63 (18.4)
Eccentric mass	139 (46.5)	169 (49.3)
Circumferential mass	107 (35.8)	111 (32.4)
Tumor length (cm), mean ± SD	4.59±0.146	4.49±0.126
Tumor location, n (%)		
Upper	41 (13.7)	39 (11.4)
Middle	114 (38.1)	138 (40.2)
Lower	144 (48.2)	166 (48.4)
Long axis (mm), n (%)		
Mean ± SD	7.60±0.185	7.98±0.163
≤10/8 mm	239 (79.9)	199 (58.0)
>10/8 mm	60 (20.1)	144 (42.0)
Short axis (mm), n (%)		
Mean ± SD	5.42±0.121	5.53±0.100
≤7.5/6.5 mm	256 (85.6)	261 (76.1)
>7.5/6.5 mm	43 (14.4)	82 (23.9)
Long-to-short-axis ratio, mean ± SD	1.41±0.017	1.45±0.017

RLN, recurrent laryngeal nerve; LN, lymph node; BMI, body mass index; CT, computed tomography; SD, standard deviation.

the multivariable analysis, we constructed a nomogram that could predict the probability of left RLN LN metastasis (see *Figure 5A*). The c-index for the nomogram was 0.7609 (0.7522–0.7636). The calibration curves showed that there was good agreement between the nomogram-predicted probability and the actual metastasis rate (see *Figure 6A*). Further, a DCA was used to compare the use of the nomogram and hypothetical all-screening or no-screening scenarios. As illustrated in *Figure 6C*, the DCA graphically shows the clinical usefulness of the model based on a continuum of potential thresholds for the left RLN LN metastasis risk (x-axis) and the net benefit of using the model to risk stratify patients (y-axis) relative to the assumption that either no patients or all patients would have left RLN LN metastasis. In this analysis, the application of the model provided net benefits with threshold probabilities of 0.017–0.725. Finally, we performed RPA for risk stratification according to the probability of left RLN LN metastasis. The tree was pruned to generate 3 subgroups for the risk of left RLN LN metastasis. As *Figure 7A* shows, tumor location and the short axis generated a tree with 2 nodes that separated the patients into the following 3 risk groups: (I) the low-risk group: patients with a short axis of left RLN LN ≤7.5 mm; (II) the intermediate-risk group: patients with lower thoracic esophagus and a short axis of left RLN LN >7.5 mm; and (III) the high-risk group: patients with upper/middle thoracic esophagus and a short axis of left RLN LN >7.5 mm. The risk of left RLN LN metastasis was 9.3%, 27.3%, and 52.4% for the low-risk, intermediate-risk, and high-risk groups, respectively (see *Figure 7A*).

Risk stratification of right RLN LN metastasis

In Cohort 2, the univariable and multivariable analyses

Table 2 Detailed information in ROC curves of left and right RLN LN metastasis

Variables	Left RLN LN			Right RLN LN		
	Long axis	Short axis	Long-to-short-axis ratio	Long axis	Short axis	Long-to-short-axis ratio
Cutoff value	10 mm	7.5 mm	–	8 mm	6.5 mm	–
AUC (95% CI)	0.682 (0.586–0.777)	0.665 (0.565–0.764)	0.553 (0.462–0.645)	0.748 (0.687–0.809)	0.750 (0.684–0.816)	0.542 (0.467–0.618)
Sensitivity	46.3%	41.5%	–	76.9%	60.0%	–
Specificity	89.5%	90.7%	–	67.3%	82.0%	–
P value	<0.001	0.001	0.274	<0.001	<0.001	0.288

ROC, receiver operating characteristic; RLN, recurrent laryngeal nerve; LN, lymph node; AUC, area under the curve; CI, confidence interval.

Page 8 of 13

Zhang et al. Risk stratification of lymph node metastasis

Table 3 Univariable analysis for risk factors of metastasis of left and right RLN LNs

Variables	Left RLN LN (n=299)		Right RLN LN (n=343)	
	HR (95% CI)	P value	HR (95% CI)	P value
Gender				
Male	Baseline		Baseline	
Female	0.760 (0.363–1.589)	0.465	0.870 (0.486–1.558)	0.639
Age	1.058 (1.011–1.108)	0.016	0.998 (0.963–1.034)	0.896
BMI	1.049 (0.944–1.166)	0.371	1.050 (0.964–1.145)	0.263
CT appearance				
Mass absent	Baseline	0.132	Baseline	0.013
Eccentric mass	1.707 (0.547–5.329)	0.357	5.224 (1.546–17.655)	0.008
Circumferential mass	2.816 (0.910–8.710)	0.072	6.429 (1.864–22.169)	0.003
Tumor length	1.027 (0.905–1.165)	0.684	1.057 (0.946–1.181)	0.327
Tumor location				
Upper	Baseline	0.037	Baseline	0.019
Middle	1.161 (0.455–2.965)	0.754	0.652 (0.296–1.435)	0.288
Lower	0.442 (0.162–1.207)	0.111	0.344 (0.152–0.776)	0.010
Long axis				
≤10/8 mm	Baseline		Baseline	
>10/8 mm	4.571 (2.273–9.193)	<0.001	6.525 (3.481–12.229)	<0.001
Short axis				
≤7.5/6.5 mm	Baseline		Baseline	
>7.5/6.5 mm	6.321 (3.010–12.272)	<0.001	5.734 (3.211–10.239)	<0.001
Long-to-short-axis ratio	2.084 (0.741–5.859)	0.164	1.574 (0.693–3.576)	0.279

RLN, recurrent laryngeal nerve; LN, lymph node; HR, hazard ratio; CI, confidence interval; BMI, body mass index; CT, computed tomography.

showed that CT appearance, tumor location, long axis, and short axis were significantly associated with right RLN LN metastasis (all P<0.05; see *Tables 3* and *4*). The c-index for the nomogram (see *Figure 5B*) was 0.7859 (0.7818–0.7909). The calibration curves showed that there was good agreement between the nomogram-predicted probability and the actual metastasis rate (see *Figure 6B*). As illustrated in *Figure 6D*, the application of the model provided net benefits with threshold probabilities of 0.05–0.623. Finally, as *Figure 7B* shows, the long axis and short axis generated a tree with 2 nodes that separated the patients into the following 3 risk groups: (I) the low-risk group: patients with a long axis of right RLN LN ≤8 mm; (II) the intermediate-risk group: patients with a long axis >8 mm and a short axis

≤6.5 mm of right RLN LN; and (III) the high-risk group: patients with a long axis >8 mm and a short axis >6.5 mm of right RLN LN. The risk of right RLN LN metastasis was 7.5%, 21.4%, and 47.3% for the low-risk, intermediate-risk, and high-risk groups, respectively (see *Figure 7B*).

Discussion

The RLN is derived from the vagus trunk. The right RLN loops under the subclavian artery. The left RLN has a long course, as it curves below and behind the aortic arch at the level of the ligamentum arteriosum. As the size of a LN might depend on the amount of lymphatic drainage from neighboring tissues and organs (10), the left and right

Table 4 Univariable and multivariable logistic regression analyses for risk factors of metastasis of left and right RLN LNs

Variables	Left RLN LN (n=299)			Right RLN LN (n=343)		
	β coefficient (SE)	HR (95% CI)	P value	β coefficient (SE)	HR (95% CI)	P value
Age	0.060 (0.0260)	1.062 (1.009–1.118)	0.022			
CT appearance						
Mass absent				Baseline	Baseline	0.028
Eccentric mass				1.660 (0.648)	5.258 (1.477–18.720)	0.010
Circumferential mass				1.737 (0.663)	5.680 (1.549–20.825)	0.009
Tumor location						
Upper	Baseline	Baseline	0.032	Baseline	Baseline	0.041
Middle	0.293 (0.525)	1.340 (0.479–3.750)	0.577	0.953 (0.478)	0.813 (0.325–2.034)	0.658
Lower	−0.790 (0.559)	0.454 (0.152–1.359)	0.158	0.746 (0.339)	0.385 (0.151–0.984)	0.046
Long axis						
≤10/8 mm				Baseline	Baseline	
>10/8 mm				1.467 (0.376)	4.336 (2.075–9.063)	<0.001
Short axis						
≤7.5/6.5 mm	Baseline	Baseline		Baseline	Baseline	
>7.5/6.5 mm	1.429 (0.574)	4.176 (1.357–12.852)	0.013	0.793 (0.355)	2.210 (1.102–4.429)	0.025

RLN, recurrent laryngeal nerve; LN, lymph node; SE, standard error; HR, hazard ratio; CI, confidence interval; CT, computed tomography.

RLN LNs may possess different anatomical characteristics and metastasis patterns. The node distribution and size patterns of the left and right RLN LNs have been described previously (12); however, the precise metastasis risk stratifications and their differences between the left and right RLN LNs have not yet been analyzed.

The accurate preoperative evaluation of LN metastasis is of vital importance for esophageal cancer staging. To date, various imaging technologies, such as CT scans, magnetic resonance imaging (MRI), fluorodeoxyglucose (FDG)-positron emission tomography (PET), endoscopic ultrasonography (EUS), EUS-fine-needle aspiration (FNA), Endobronchial Ultrasound (EBUS), and EBUS-guided transbronchial needle aspiration (EBUS-TBNA), have made different levels of contribution to the preoperative diagnosis of LN metastasis. MRI has better diagnostic performance for characterizing benign or malignant LNs (29,30); however, it is a time-consuming and relatively expensive examination. FDG-PET can detect metastatic LNs that are not enlarged in size; however, its specificity in evaluating regional LN metastasis is high with low sensitivity (31). Compared to CT, EBUS and EUS had significantly superior sensitivity, whereas CT had significantly superior specificity

(32,33). The accuracy of detecting LN metastases by EUS-FNA and EBUS-TBNA is high; however, the method is invasive and technically challenging to apply in the RLN area; furthermore, biopsy may cause postprocedural hematomas around the LN, which may increase the risk of RLN injury during LN dissection. Thus, EUS-FNA and EBUS-TBNA are unsuitable for routine use (32,34). High-resolution CT scans are the routine method for assessing tumor resectability at our center, and in this study, we used CT scans to detect abnormal LNs. The detection of metastatic LNs in CT is generally based on size criteria; short axes of LNs >10 mm are judged as metastatic. Li *et al.* demonstrated that a smaller 6.5 mm cutoff value of the short axis can be applied to predict LN metastasis (18). Recently, an even smaller 5 mm cutoff value of the short axis was adopted by Liu *et al.* (16). However, some LNs can reach a considerable size as a result of a reaction to benign inflammation, and those less than the cutoff value are often malignant. Given that LN metastasis is associated with many factors, we included various preoperative factors to investigate the risk of RLN LN metastasis.

Interestingly, we found that LN shape evaluated by the long-to-short-axis ratio had no predictive value for left and

Page 10 of 13

Zhang et al. Risk stratification of lymph node metastasis

right RLN LN metastasis. Our results appear to differ to those of Liu *et al.*, who proposed that a 1.52 cutoff value of the long-to-short axis ratio was clinically significant (and round LNs were more likely to be metastatic) (15), which suggests the particularity of the left and right RLN LNs. As *Table 1* shows, the median long-axis, short-axis and long-to-short-axis ratios of the left (right) RLN LNs were 7.60±0.185 mm (7.98±0.163 mm), 5.42±0.121 mm (5.53±0.100 mm), and 1.41±0.017 (1.45±0.017), respectively. Thus, the right RLN LNs appeared to be larger and flatter. Additionally, the cutoff values of the long axis and short axis for predicting metastasis of the left (right) RLN LNs were 10 mm (8 mm) and 7.5 mm (6.5 mm), respectively. At the same time, another question arises: Which is more important: the long axis or the short axis? In our study, the multivariable analysis showed that the short axis rather than the long axis was significantly associated with left RLN LN metastasis. Similarly, the long axis was much more important than the short axis in relation to the right RLN LNs (hazard rato (HR) =4.336 for the long axis and HR =2.210 for the short axis). The reason for this inconsistent conclusion may be due to the anatomical differences between the left and right RLN LNs. However, the prediction value of the single long- or short-axis factor is limited with low sensitivity values (see *Table 2*), which is consistent with previous studies (15,35).

Studies have shown that the rates of bilateral RLN LN metastasis for upper esophageal tumors were the highest, followed by middle and lower esophageal tumors (6,13,36). However, in our study, we found that there were still differences between the left and right RLN LN metastases. As *Table 4* shows, there was a higher incidence of right RLN LN metastasis in patients with upper thoracic esophageal tumors. For the left RLN LNs, the middle esophageal tumors had the highest metastasis rate. The reason for the difference may be related to different definitions of tumor location. To date, there are 2 main classification definitions of tumor location; that is, the definition under the Japanese Classification of Esophageal Cancer system and the definition under the AJCC system (19,20). According to the Japanese Classification of Esophageal Cancer system, the proximal or distal half of the 2 equal portions between the tracheal bifurcation and the esophagogastric junction was defined as the middle or lower thoracic esophagus. According to the AJCC system, there is a great difference in length between the middle and the lower thoracic esophagus (middle thoracic esophagus, 25–30 cm; lower thoracic esophagus, 30–40 cm). Further,

we demonstrated that our proposed radiological appearance can significantly predict right RLN LN metastasis, with type 3 (circumferential mass) having the highest increased risks (HR =5.680). However, no significant difference of left RLN LN metastasis among radiological appearances was found. Similarly, this can be explained by the lymphatic drainage pattern of the esophagus. The right RLN LNs are located very close to the superior portion of the right paratracheal chain and receive lymphatics from almost all levels of the esophagus, while the left RLN LNs receive lymphatics from lower levels of the esophagus. Thus, the right RLN LNs are more likely to be affected by the tumor invasiveness of the esophageal wall than the left RLN LNs.

To make accurate predictions of left and right RLN LNs, we included significant preoperative variables in our nomograms. Finally, we stratified the cohorts into several risk subgroups to help clinicians select more effective treatment strategies. According to our results, all of the risk factors need to be taken into consideration when making stratifications to obtain more accurate results. For example, left RLN LNs with short axes >7.5 mm may be placed in the intermediate-risk or high-risk group according to the different tumor locations. Similarly, right RLN LNs with a long axis >8 mm may be placed in the intermediate-risk or high-risk group because they are also affected by the short axis.

Our stratification model showed reasonable accuracy in predicting left and right RLN LN metastasis; however, care should be taken when using our stratification model for counseling. The preoperative prediction of LN status is challenging, and 100% accurate predictions of LN metastasis cannot be made preoperatively. To determine the probability of LN metastasis as accurately as possible, additional preoperative parameters, such as preoperative tumor markers, should be introduced into the prediction model. Second, it is possible that the lack of data regarding the environment or lifestyle of the patients led to the moderate c-index that was observed in our stratification model. Third, we were unable to conduct independent external validation with different patient populations from other centers. Forth, while some patients had multiple RLN LNs, we could only take the largest LN into account when calculating the long and short axes. Thus, the preoperative CT diagnosis of a LN may not correspond to the proper site of surgical removal and postoperative pathological diagnosis of the LN. Last but not least, the study's retrospective design bring many uncertainties. Specifically, selection bias was unavoidable. Aiming to control selection bias, strict inclusion and exclusion criteria

were applied. Also, esophageal cancer related definitions (such as clinical or pathological stage, tumor location) had changed. So we collected data based on uniform definitions to provide consistent data for analysis.

In conclusion, our nomograms and RPAs appear to be suitable for the risk stratification of left and right RLN LN metastasis in patients undergoing thoracolaparoscopic esophagectomy with cervical anastomosis using a relatively large cohort. This tool could be used to help clinicians select more effective locoregional treatments, such as surgical protocols and radiation area selections.

Footnote

Reporting Checklist: The authors have completed the TRIPOD reporting checklist. Available at https://dx.doi.org/10.21037/atm-21-2374

Data Sharing Statement: Available at https://dx.doi.org/10.21037/atm-21-2374

Conflicts of Interest: All authors have completed the ICMJE uniform disclosure form (available at https://dx.doi.org/10.21037/atm-21-2374). The authors have no conflicts of interest to declare.

Ethical Statement: The authors are accountable for all aspects of the work in ensuring that questions related to the accuracy or integrity of any part of the work are appropriately investigated and resolved. All procedures performed in this study involving human participants were in accordance with the Declaration of Helsinki (as revised in 2013). This study was deemed exempt from review by the Zhengzhou University Institutional Review Board (No.: 2021-KY-0397-102) and informed consent was waived because our study was retrospective.

Open Access Statement: This is an Open Access article distributed in accordance with the Creative Commons

References

1. Wu J, Chen QX, Zhou XM, et al. Does recurrent laryngeal nerve lymph node metastasis really affect the prognosis in node-positive patients with squamous cell carcinoma of the middle thoracic esophagus? BMC Surg 2014;14:43.
2. Ye K, Xu JH, Sun YF, et al. Characteristics and clinical significance of lymph node metastases near the recurrent laryngeal nerve from thoracic esophageal carcinoma. Genet Mol Res 2014;13:6411-9.
3. Taniyama Y, Miyata G, Kamei T, et al. Complications following recurrent laryngeal nerve lymph node dissection in oesophageal cancer surgery. Interact Cardiovasc Thorac Surg 2015;20:41-6.
4. Malassagne B, Tiret E, Duprez D, et al. Prognostic value of thoracic recurrent nerve nodal involvement in esophageal squamous cell carcinoma. J Am Coll Surg 1997;185:244-9.
5. Li H, Yang S, Zhang Y, et al. Thoracic recurrent laryngeal lymph node metastases predict cervical node metastases and benefit from three-field dissection in selected patients with thoracic esophageal squamous cell carcinoma. J Surg Oncol 2012;105:548-52.
6. Shiozaki H, Yano M, Tsujinaka T, et al. Lymph node metastasis along the recurrent nerve chain is an indication for cervical lymph node dissection in thoracic esophageal cancer. Dis Esophagus 2001;14:191-6.
7. Lee PC, Port JL, Paul S, et al. Predictors of long-term survival after resection of esophageal carcinoma with nonregional nodal metastases. Ann Thorac Surg 2009;88:186-92; discussion 192-3.
8. Chao YK, Chiu CH, Liu YH. Safety and oncological efficacy of bilateral recurrent laryngeal nerve lymph-node dissection after neoadjuvant chemoradiotherapy in esophageal squamous cell carcinoma: a propensity-matched analysis. Esophagus 2020;17:33-40.
9. Matsubara T, Ueda M, Nagao N, et al. Cervicothoracic approach for total mesoesophageal dissection in cancer of the thoracic esophagus. J Am Coll Surg 1998;187:238-45.
10. Wang Y, Zhu L, Xia W, et al. Anatomy of lymphatic

Page 12 of 13

Zhang et al. Risk stratification of lymph node metastasis

drainage of the esophagus and lymph node metastasis of thoracic esophageal cancer. Cancer Manag Res 2018;10:6295-303.

11. Xu J, Zheng B, Zhang S, et al. The clinical significance of the intraoperative pathological examination of bilateral recurrent laryngeal nerve lymph nodes using frozen sections in cervical field lymph node dissection of thoracic esophageal squamous cell carcinoma. J Thorac Dis 2019;11:3525-33.

12. Kanemura T, Makino T, Miyazaki Y, et al. Distribution patterns of metastases in recurrent laryngeal nerve lymph nodes in patients with squamous cell esophageal cancer. Dis Esophagus 2017;30:1-7.

13. Udagawa H, Ueno M, Shinohara H, et al. The importance of grouping of lymph node stations and rationale of three-field lymphoadenectomy for thoracic esophageal cancer. J Surg Oncol 2012;106:742-7.

14. Gore RM. Upper gastrointestinal tract tumours: diagnosis and staging strategies. Cancer Imaging 2005;5:95-8.

15. Liu J, Wang Z, Shao H, et al. Improving CT detection sensitivity for nodal metastases in oesophageal cancer with combination of smaller size and lymph node axial ratio. Eur Radiol 2018;28:188-95.

16. Liu Y, Zou ZQ, Xiao J, et al. A nomogram prediction model for recurrent laryngeal nerve lymph node metastasis in thoracic oesophageal squamous cell carcinoma. J Thorac Dis 2019;11:2868-77.

17. Yu S, Lin J, Chen C, et al. Recurrent laryngeal nerve lymph node dissection may not be suitable for all early stage esophageal squamous cell carcinoma patients: an 8-year experience. J Thorac Dis 2016;8:2803-12.

18. Li B, Li B, Jiang H, et al. The value of enhanced CT scanning for predicting lymph node metastasis along the right recurrent laryngeal nerve in esophageal squamous cell carcinoma. Ann Transl Med 2020;8:1632.

19. Society JE. Japanese Classification of Esophageal Cancer, 11th Edition: part I. Esophagus 2017;14:1-36.

20. Society JE. Japanese Classification of Esophageal Cancer, 11th Edition: part II and III. Esophagus 2017;14:37-65.

21. Silveira JV, Junqueira FP, Silveira CG, et al. Kommerell Diverticulum: Right Aortic Arch with Anomalous Origin of Left Subclavian Artery and Duplicity of Right Vertebral Artery in a 16-Year-Old Girl. Am J Case Rep 2019;20:228-32.

22. Saito T, Tamatsukuri Y, Hitosugi T, et al. Three cases of retroesophageal right subclavian artery. J Nippon Med Sch 2005;72:375-82.

23. Mizowaki T, Nishimura Y, Shimada Y, et al. Optimal size criteria of malignant lymph nodes in the treatment planning of radiotherapy for esophageal cancer: evaluation by computed tomography and magnetic resonance imaging. Int J Radiat Oncol Biol Phys 1996;36:1091-8.

24. Pertl L, Zacherl J, Mancusi G, et al. High risk of unilateral recurrent laryngeal nerve paralysis after esophagectomy using cervical anastomosis. Eur Arch Otorhinolaryngol 2011;268:1605-10.

25. Gockel I, Kneist W, Keilmann A, et al. Recurrent laryngeal nerve paralysis (RLNP) following esophagectomy for carcinoma. Eur J Surg Oncol 2005;31:277-81.

26. Baba M, Natsugoe S, Shimada M, et al. Does hoarseness of voice from recurrent nerve paralysis after esophagectomy for carcinoma influence patient quality of life? J Am Coll Surg 1999;188:231-6.

27. Booka E, Takeuchi H, Nishi T, et al. The Impact of Postoperative Complications on Survivals After Esophagectomy for Esophageal Cancer. Medicine (Baltimore) 2015;94:e1369.

28. R Core Team. R: A Language and Environment for Statistical Computing. 2019. R Foundation for Statistical Computing, Vienna, Austria. Available online at https://www.R-project.org/

29. Nishimura H, Tanigawa N, Hiramatsu M, et al. Preoperative esophageal cancer staging: magnetic resonance imaging of lymph node with ferumoxtran-10, an ultrasmall superparamagnetic iron oxide. J Am Coll Surg 2006;202:604-11.

30. Shuto K, Kono T, Shiratori T, et al. Diagnostic performance of diffusion-weighted magnetic resonance imaging in assessing lymph node metastasis of esophageal cancer compared with PET. Esophagus 2020;17:239-49.

31. Okada M, Murakami T, Kumano S, et al. Integrated FDG-PET/CT compared with intravenous contrast-enhanced CT for evaluation of metastatic regional lymph nodes in patients with resectable early stage esophageal cancer. Ann Nucl Med 2009;23:73-80.

32. Fu X, Wang F, Su X, et al. Endobronchial Ultrasound Improves Evaluation of Recurrent Laryngeal Nerve Lymph Nodes in Esophageal Squamous Cell Carcinoma Patients. Ann Surg Oncol 2021;28:3930-8.

33. Shan HB, Zhang R, Li Y, et al. Application of Endobronchial Ultrasonography for the Preoperative Detecting Recurrent Laryngeal Nerve Lymph Node Metastasis of Esophageal Cancer. PLoS One 2015;10:e0137400.

34. Vazquez-Sequeiros E, Norton ID, Clain JE, et al. Impact of EUS-guided fine-needle aspiration on lymph node

staging in patients with esophageal carcinoma. Gastrointest Endosc 2001;53:751-7.

35. Ohi M, Toiyama Y, Yasuda H, et al. Preoperative computed tomography predicts the risk of recurrent laryngeal nerve paralysis in patients with esophageal cancer undergoing thoracoscopic esophagectomy in the prone position. Esophagus 2021;18:228-38.

36. Tachimori Y, Ozawa S, Numasaki H, et al. Efficacy of lymph node dissection by node zones according to tumor location for esophageal squamous cell carcinoma. Esophagus 2016;13:1-7.